



XXVI DAE-BRNS HIGH ENERGY PHYSICS SYMPOSIUM 2024



# From Microquasars to AGNs: An uniform Jet Variability



**Ajay Sharma**

Senior Research Fellow

(Department of Physics of Complex Systems)

S.N. Bose National Centre For Basic Sciences

# Outline

- \* **Objective**
- \* **What are Microquasars and Active Galactic Nuclei ?**
- \* **Why is investigation of gamma rays so important?**
- \* **Methods**
- \* **Results**
- \* **Conclusion**
- \* **Acknowledgement**

# Motivation

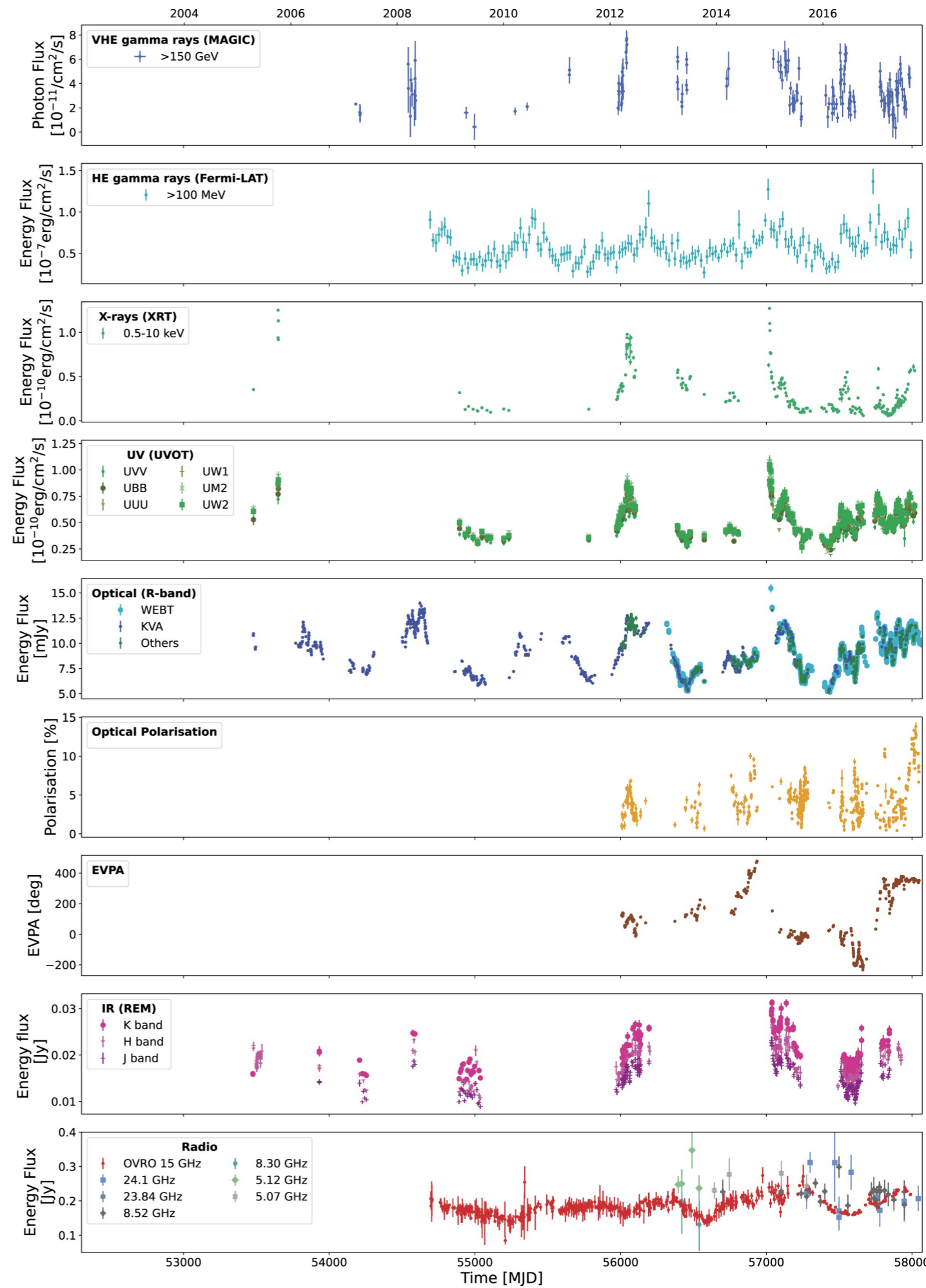
The variability study of AGN and Microquasars using multi wavelength data is a powerful tool to:

- \*Probe their structure and physical processes.
- \*Understand accretion physics and jet dynamics.
- \*Test relativistic effects near compact objects.
- \*Estimate black hole masses and study cosmic AGN evolution.

By observing variability across different timescales and wavelengths, we gain critical insights into the nature of microquasars and AGNs, their environments, and their role in the universe.

# Long-term PG 1553+113 MW. lightcurves

# H. Abe et al. 2024



# What is **Microquasar** ?

What is **Microquasar** ?



# Microquasar

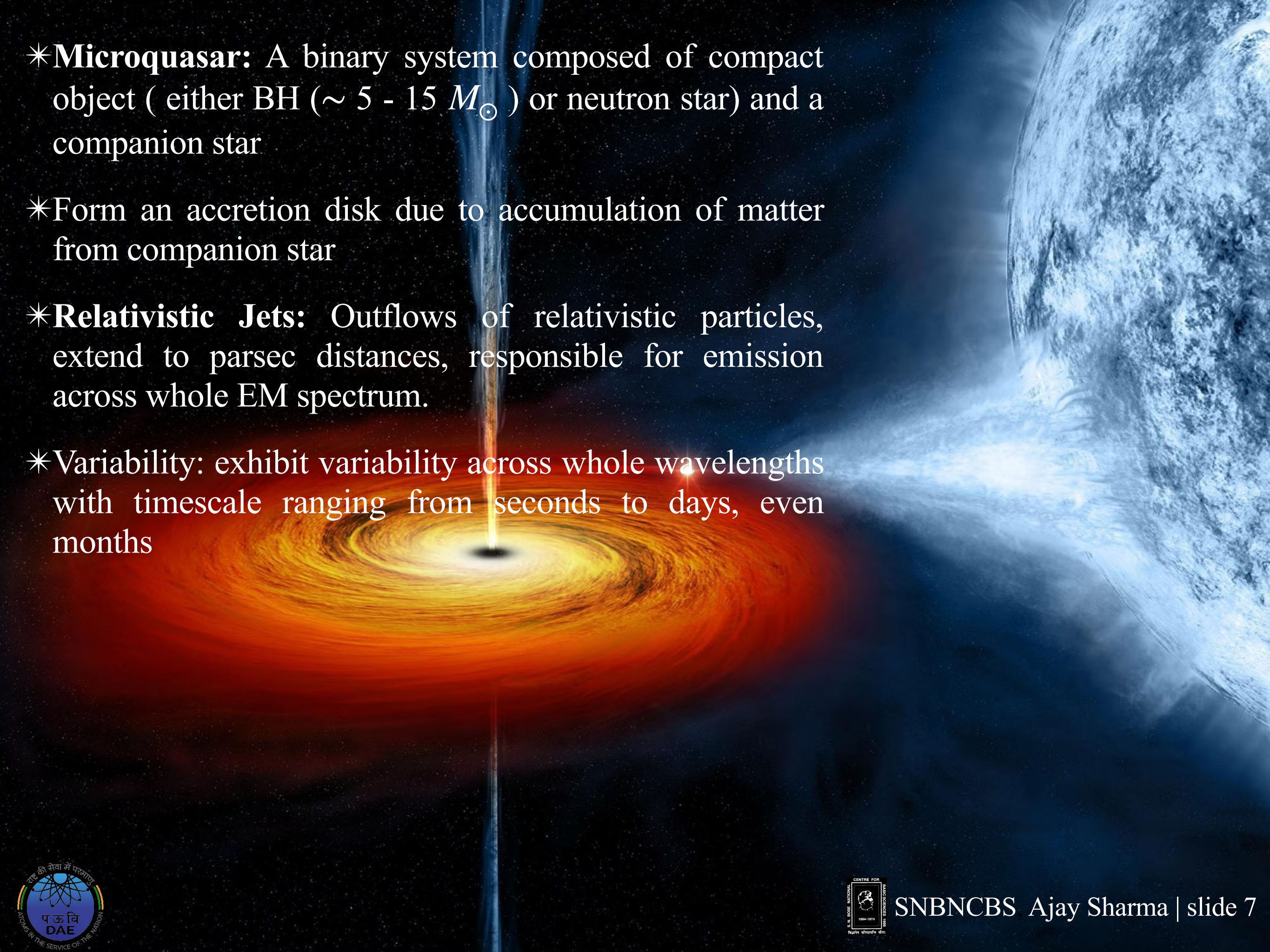
← **Relativistic Jet**

**Spinning compact object**

**Companion Star**

**Accretion disk**



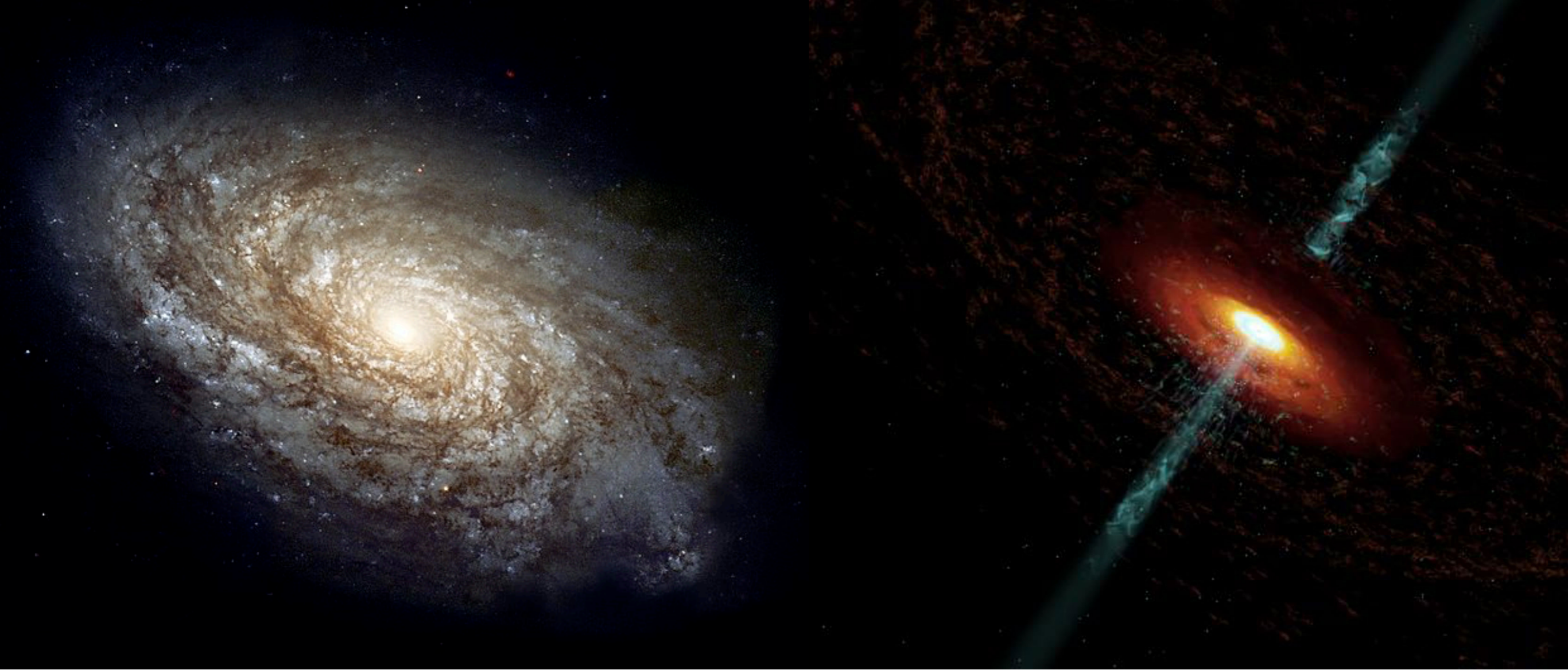
- 
- \***Microquasar:** A binary system composed of compact object ( either BH ( $\sim 5 - 15 M_{\odot}$ ) or neutron star) and a companion star
- \*Form an accretion disk due to accumulation of matter from companion star
- \***Relativistic Jets:** Outflows of relativistic particles, extend to parsec distances, responsible for emission across whole EM spectrum.
- \***Variability:** exhibit variability across whole wavelengths with timescale ranging from seconds to days, even months



# What are the Galaxies ?

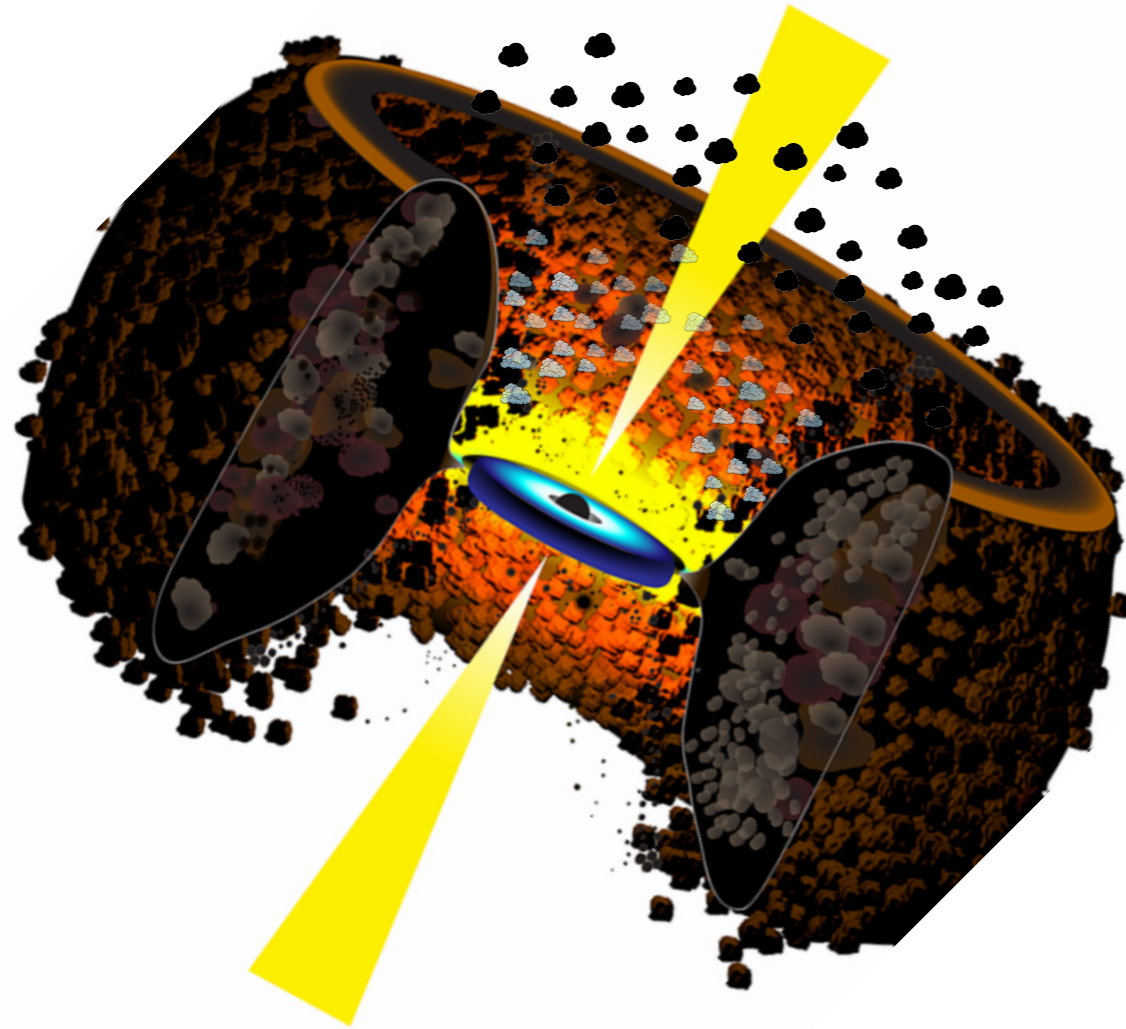
क्या हैं वे आकाशगंगाएँ ?





Normal Galaxy	Active Galaxy
It has a dormant SMBH at its center which is not accreting matter from its surroundings	Active supermassive black hole at the center of galaxy, accreting matter from its surrounding due to its high gravitational field.

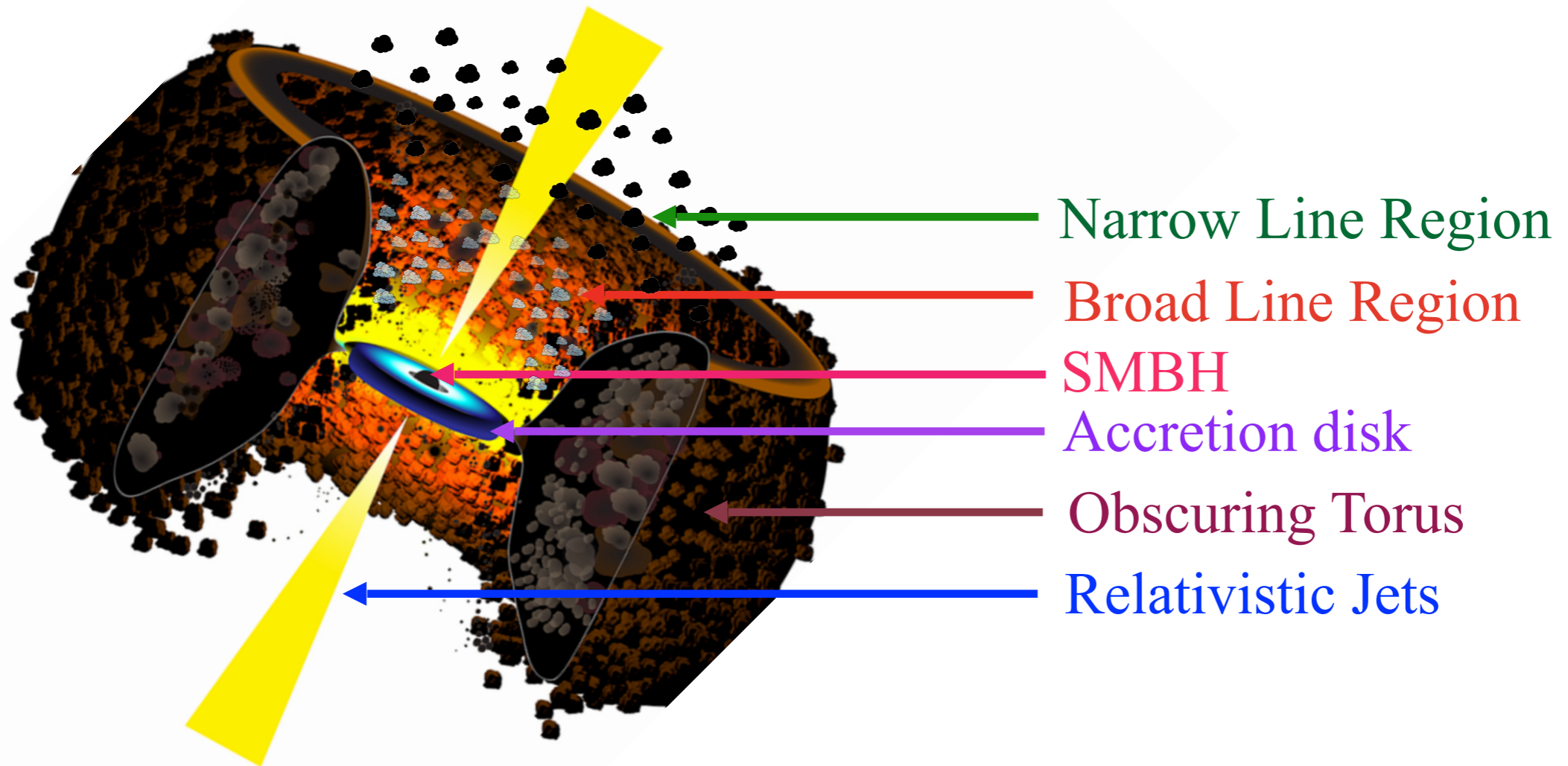
# Active galactic nuclei (AGN)



- \* AGN's are powered by the Accretion on to SMBH
- \* Highly energetic manifestations from the nuclei of galaxies, emits a prodigious amount of radiation in the form of radio, optical, x-rays,  $\gamma$ -rays and high-speed particle jet.
- \* AGN's are the most luminous persistent sources of electromagnetic radiation in the universe.
- \* The luminosity of the AGN is typically  
 $L_{AGN} \simeq 10^{13}L_{\odot} \simeq 4 \times 10^{46} \text{ergs}^{-1}$
- \* AGN's with the highest observed luminosities are expected to have BH masses of up to

$$M_{BH} \sim 10^9 - 10^{10} M_{\odot}$$

# Basic components of AGN

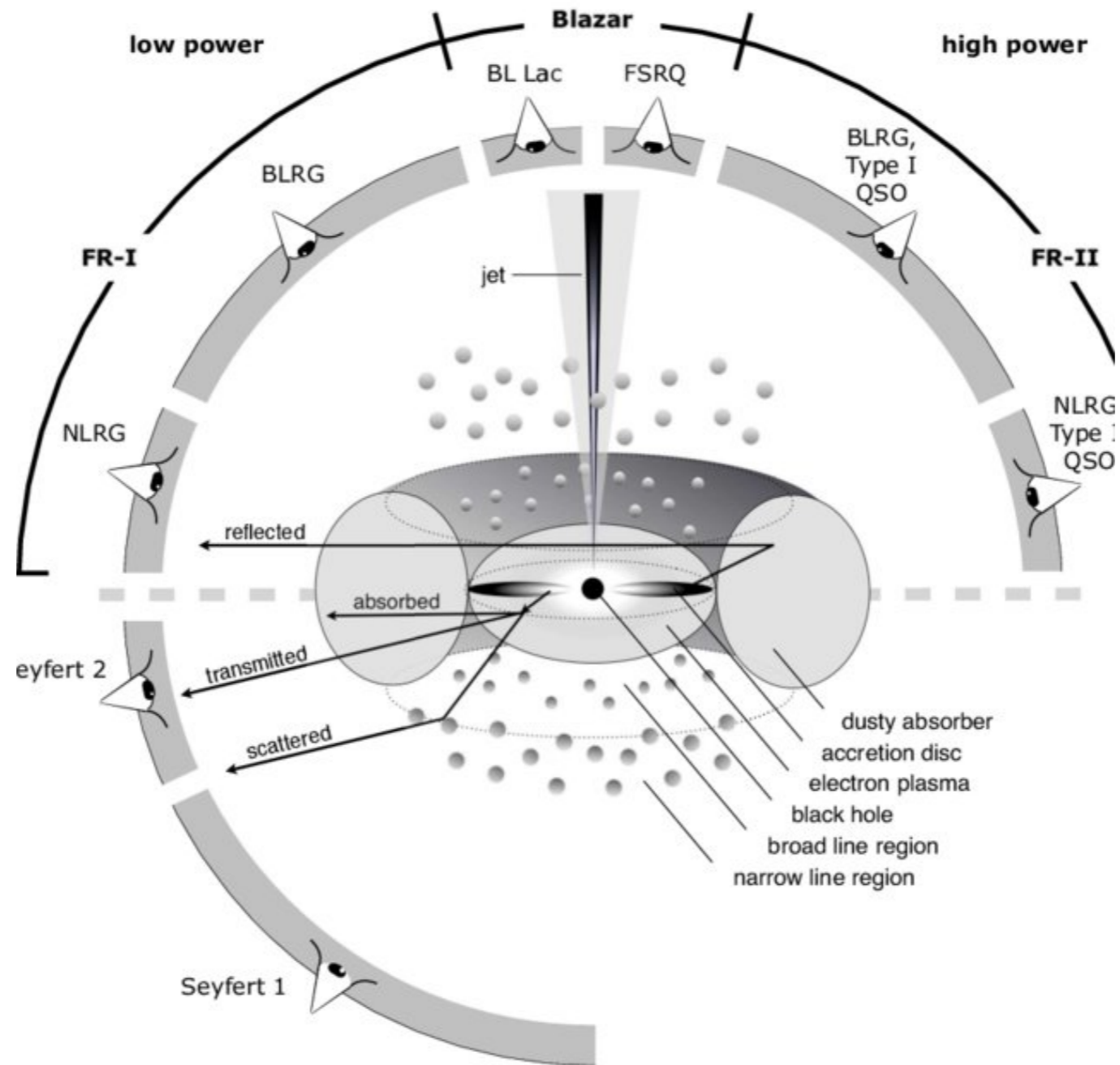


# AGN Classification

AGN Classification



# AGN Unification Scheme



Based on the orientation angle of AGN's with respect to the observer

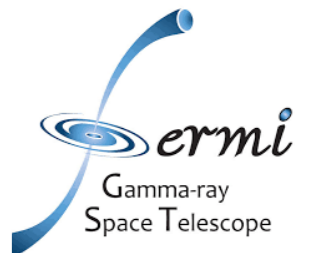
# Beckmann et al. 2012

# Similarities b/w Microquasars and AGNs

Property	Microquasar	AGN
Power Source	Stellar-mass black hole or neutron star	Supermassive black hole at the center of galaxy
Accretion Disk	Forms from the binary companion star	Forms from surrounding galactic material
Relativistic Jets	Extends up to few light-year distances, emit from radio to VHE gamma-rays, even more higher	Up to millions of light-year distances, emit radiation from radio to VHE gamma-rays, cosmic-rays, neutrinos
Emission process	<b>Thermal radiation:</b> Accretion disk, companion star <b>Non-thermal radiation:</b> From Relativistic jets via synchrotron, inverse-compton processes	<b>Thermal radiation:</b> Accretion disk, BLR, NLR, Dusty torus <b>Non-thermal radiation:</b> From Relativistic jets via synchrotron, inverse-compton processes
Variability timescale	Seconds to months	Days to years



# Source of information

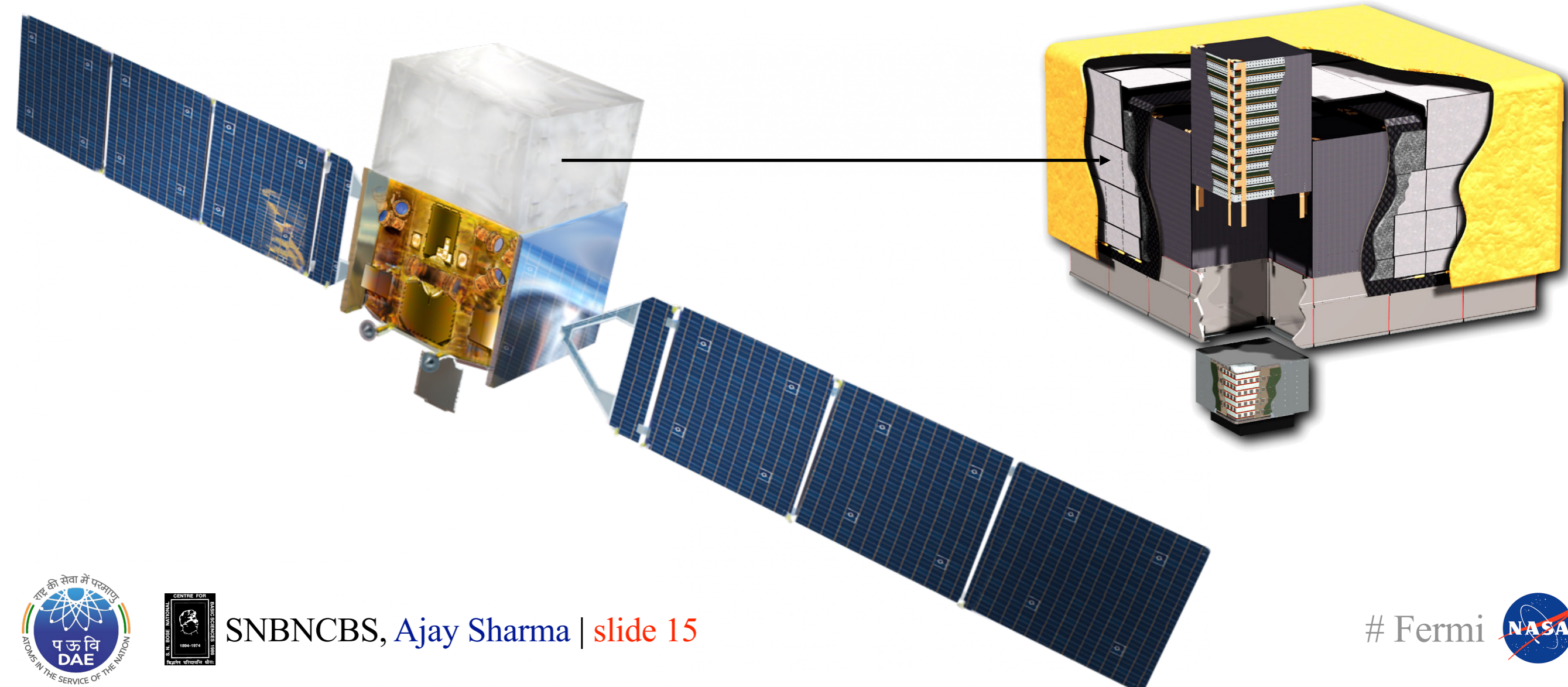


## Fermi Gamma-ray space based telescope

- \* Launched by NASA in 2008
- \* Energy coverage : from few keV upto 300GeV
- \* Scanning whole the sky in every 3 hours

### Large Area Telescope (LAT)

- FoV: 2.5 sr
- Energy range: below 100MeV upto 300GeV





# Let's discuss about variability

# Methodology

There are several different methods that can be used to investigate the temporal behaviour, such as

- Fractional Variability study
- Structure function
- Power spectral density analysis
- Gaussian Process modeling

# Gaussian Process Modelling

- ◆ Gaussian process model is CARMA(p, q), defined as the solutions to the following stochastic differential equation:

$$\frac{d^p y(t)}{dt^p} + \alpha_{p-1} \frac{d^{p-1} y(t)}{dt^{p-1}} + \dots + \alpha_0 y(t) = \beta_q \frac{d^q \epsilon(t)}{dt^q} + \beta_{q-1} \frac{d^{q-1} \epsilon(t)}{dt^{q-1}} + \dots + \beta_0 \epsilon(t)$$

## Damped Random Walk (DRW)

- ◆ Let's set p=1, q=0, i.e. a CAR(1) model, Damped Random Walk model, and also known as Ornstein-Uhlenbeck process, stochastic differential has following form :

$$\left[ \frac{d}{dt} + \frac{1}{\tau_{DRW}} \right] y(t) = \sigma_{DRW} \epsilon(t) \quad \text{Where, } \tau_{DRW} \text{ the damping timescale of DRW process,}$$

$\sigma_{DRW}$  the amplitude of random perturbations.

- ◆ DRW Kernel:  $k(t_i, t_j) = \sigma^2 \exp\left(-\frac{t_i - t_j}{\tau}\right)$ ,  $\sigma, \tau$  amplitude and damping timescale

- ◆ PSD form for the DRW process:  $S(\omega) = \sqrt{\frac{2}{\pi}} \frac{a}{c} \frac{1}{1 + \left(\frac{\omega}{c}\right)^2}$ , Where,  $a = 2\sigma_{DRW}^2$  and  $c = \frac{1}{\tau_{DRW}}$

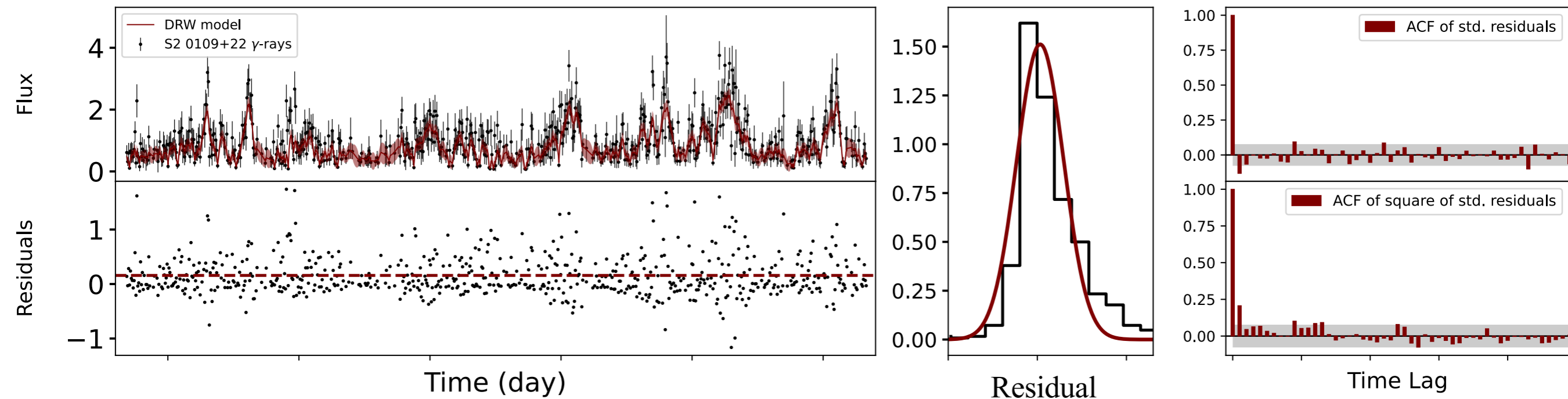
## From Microquasars to AGNs: Variability study

- \* In this investigation, we studied 13 sources, including 7 blazars, 1 radio galaxy, 1 narrow line seyfert 1 galaxy, 2 unclassified blazar candidates, and 2 microquasars.
- \* In this study, we used gamma-ray data taken by Fermi-LAT satellite.
- \* Duration of observation is  $\sim 15$  years

# DRW modeling

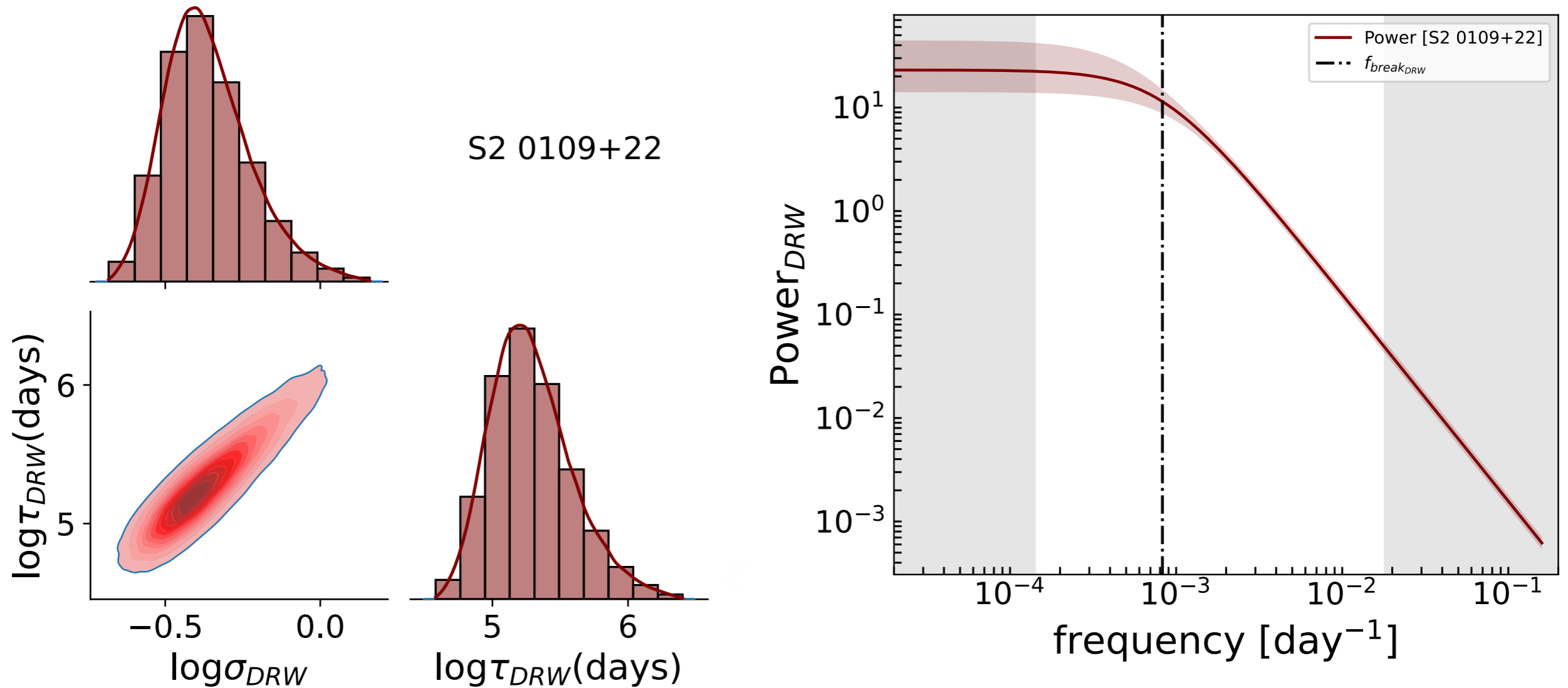
## \* DRW modeled 7-day binned gamma-ray lightcurve of blazar S2 0109+22

- Source type: BL lac
- Gal. Coord. : (129.142, -39.878)
- Redshift : 0.265



# DRW modeling

\* DRW power spectral density (PSD) profile and marginal posterior parameter distribution (MCMC) :-



## The observed parameters:

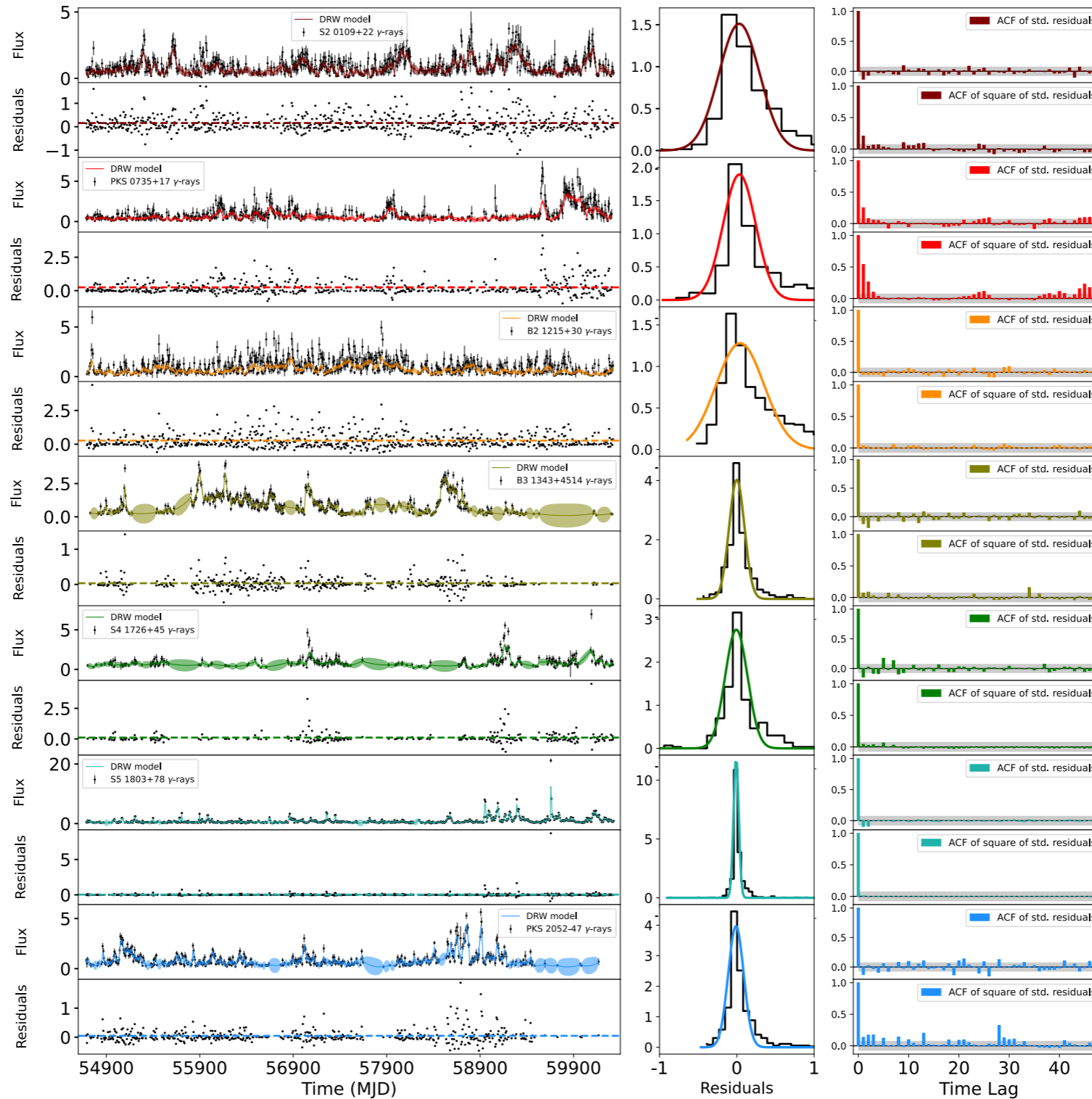
- $\log \sigma_{DRW} = -0.38^{+0.15}_{-0.12}$
- $\log \tau_{DRW_{obs. frame}} (days) = 5.26^{+0.33}_{-0.26}$
- $\log \tau_{DRW_{rest frame}} (days) = 2.67^{+0.14}_{-0.11}$

## Criteria for DRW PSD:

- $\tau_{DRW} < 0.1 \times \text{baseline}$
- $\tau_{DRW} > \text{mean cadence}$

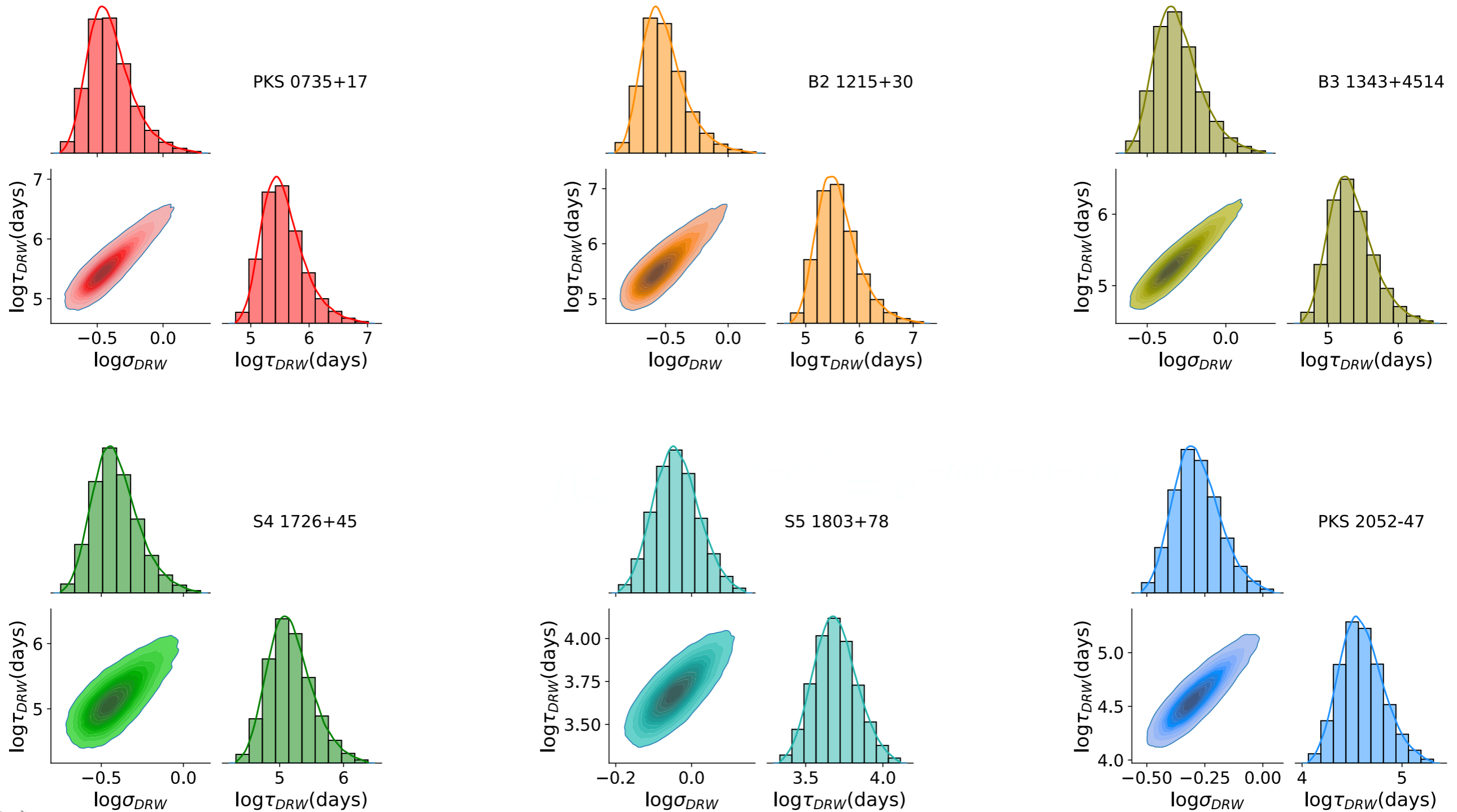
# DRW modeling

\* Modelled gamma-ray light curves of blazars:



# DRW modeling

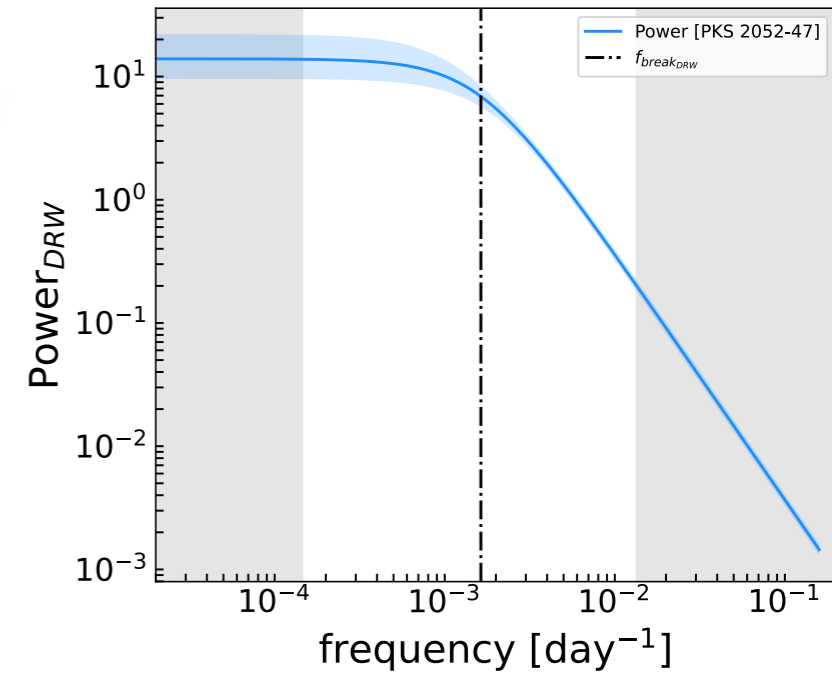
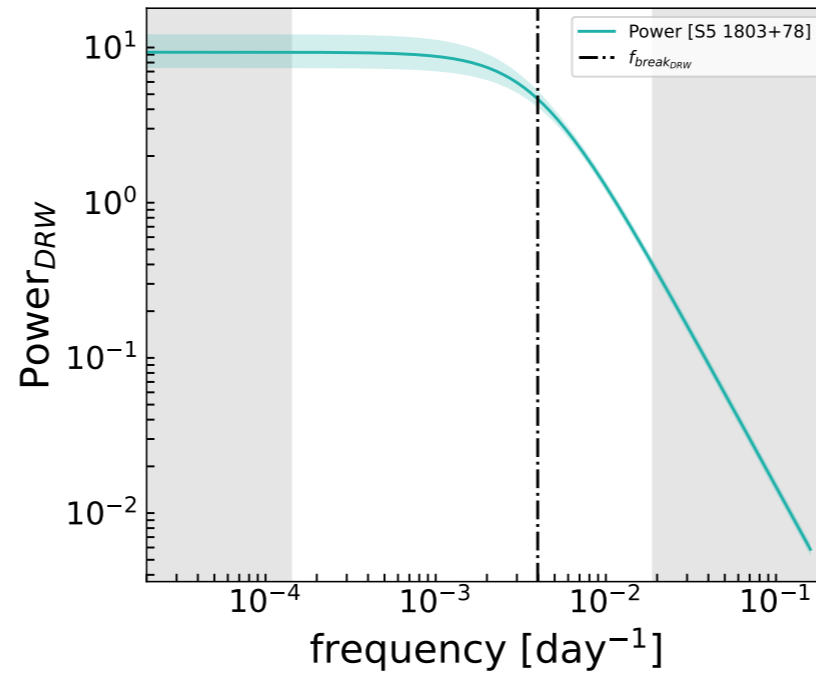
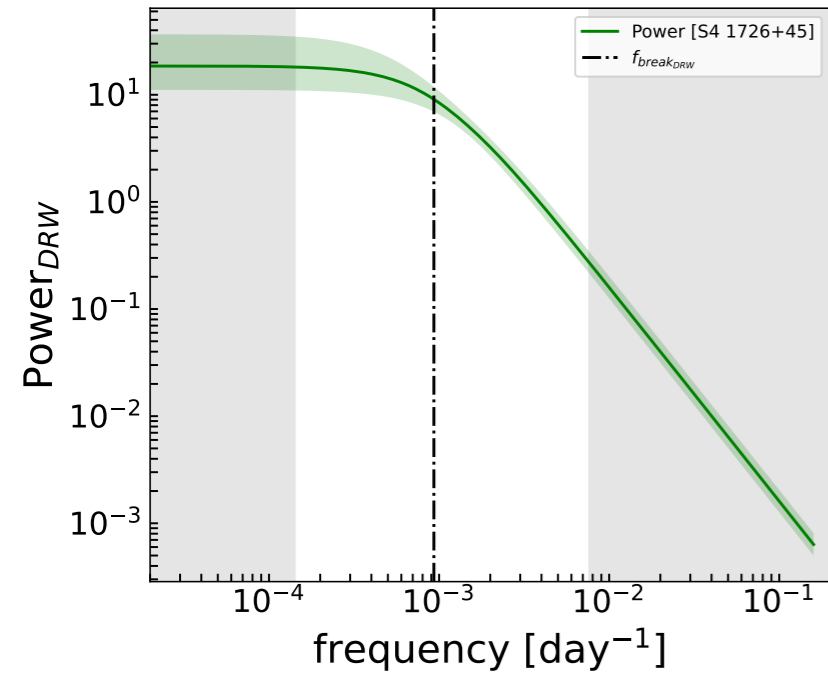
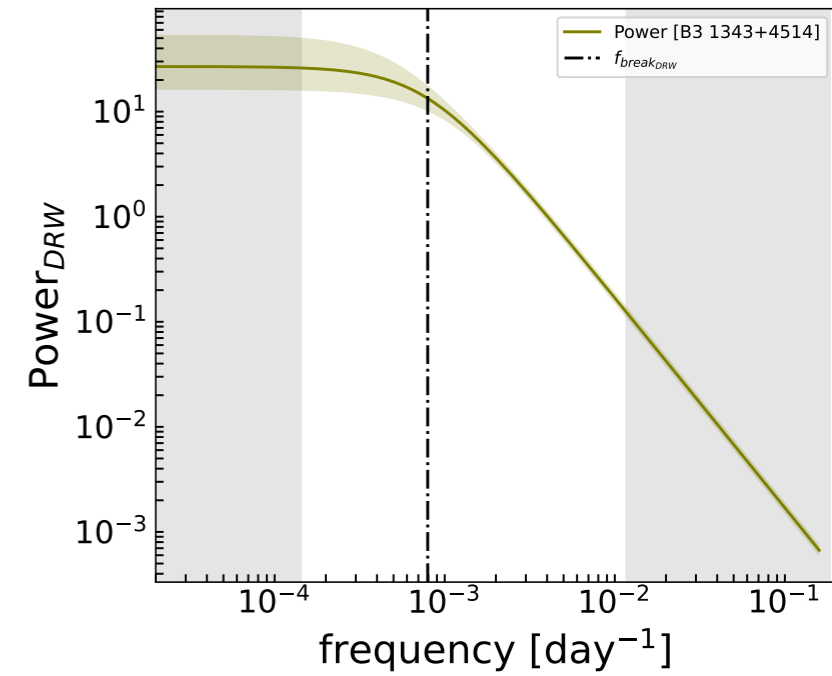
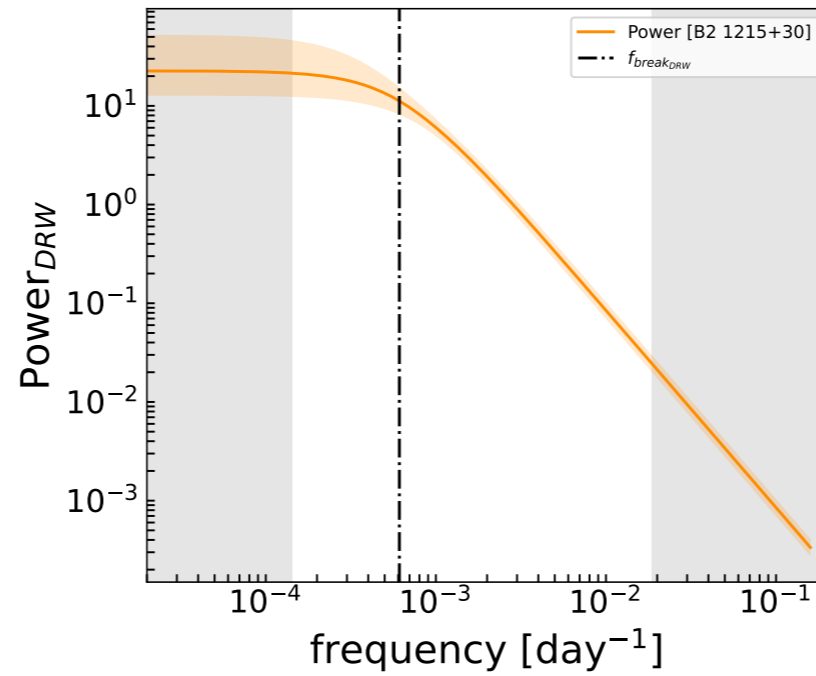
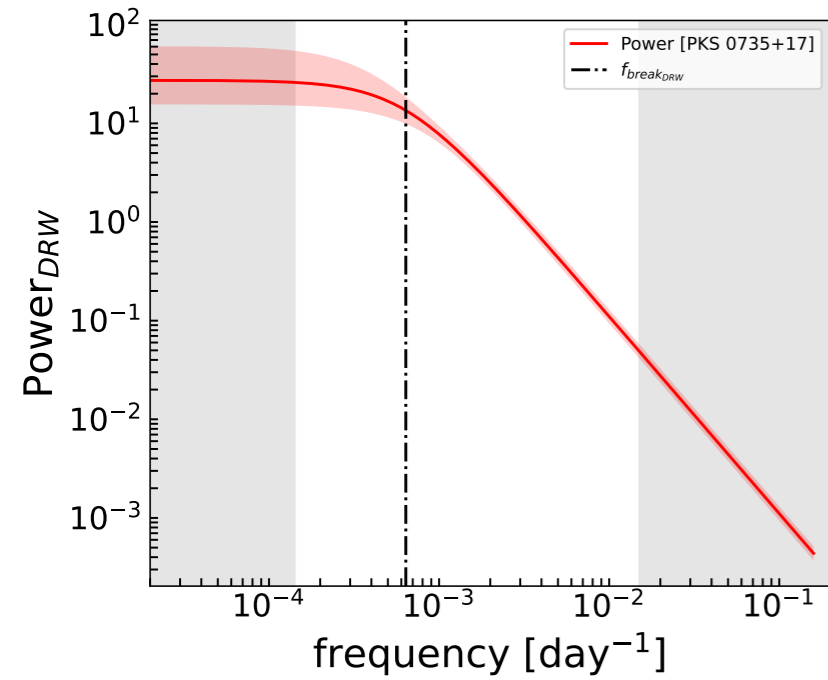
\* Marginal posterior parameter distributions of blazars:-





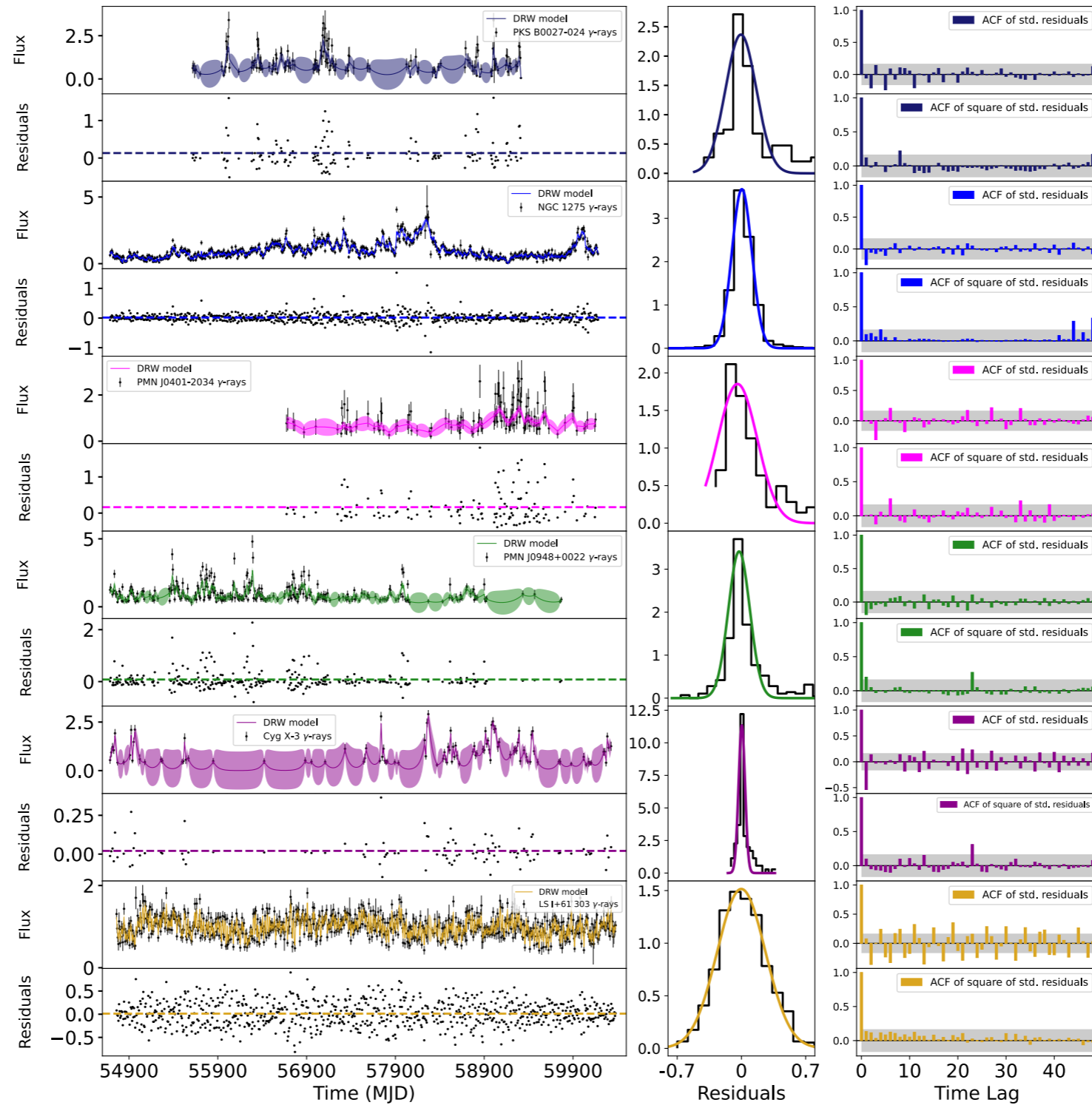
# DRW modeling

\* DRW PSD profiles of blazars :-



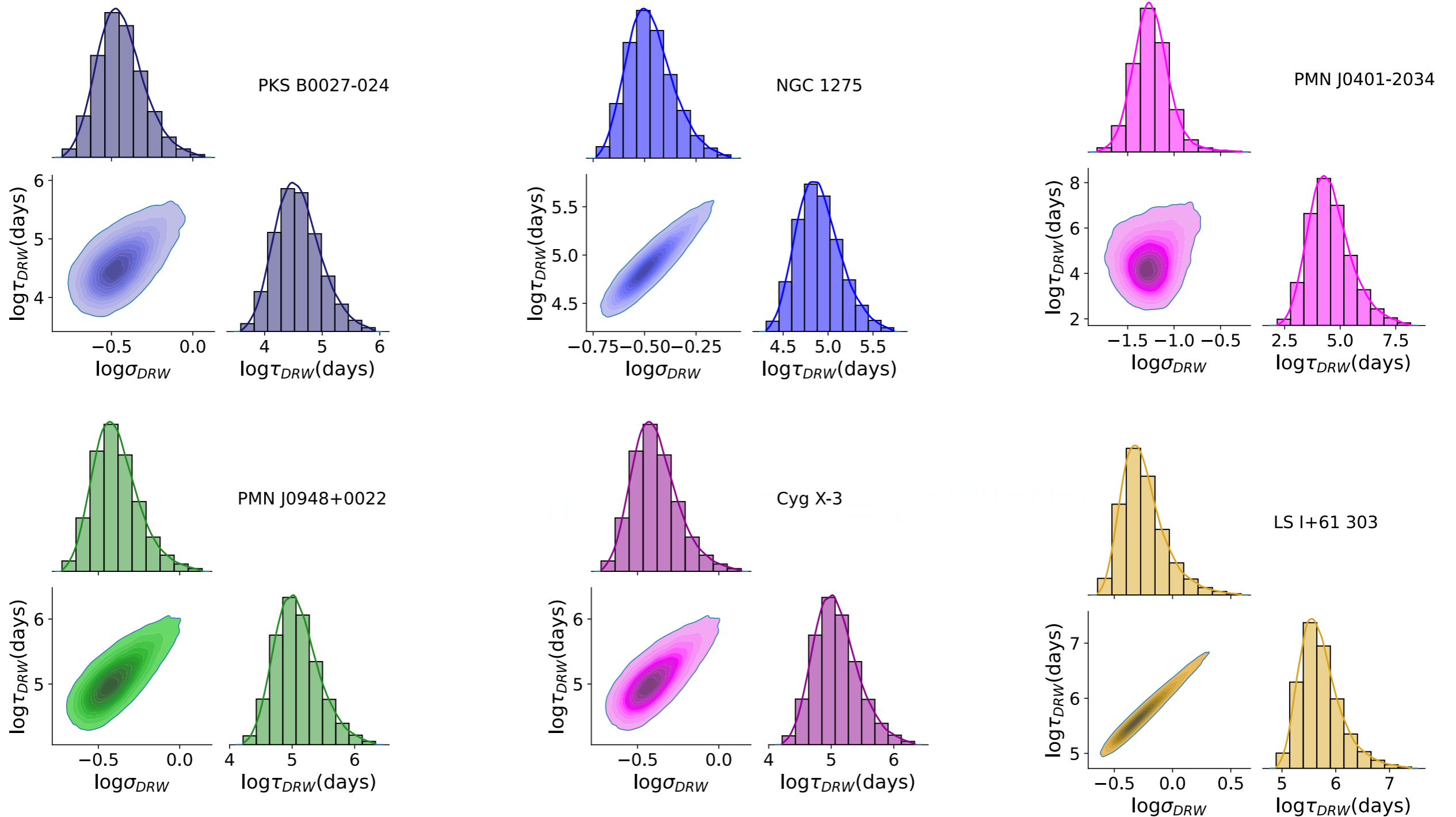
# DRW modeling

\* Modelled gamma-ray light curves of non-blazars and microquasars:



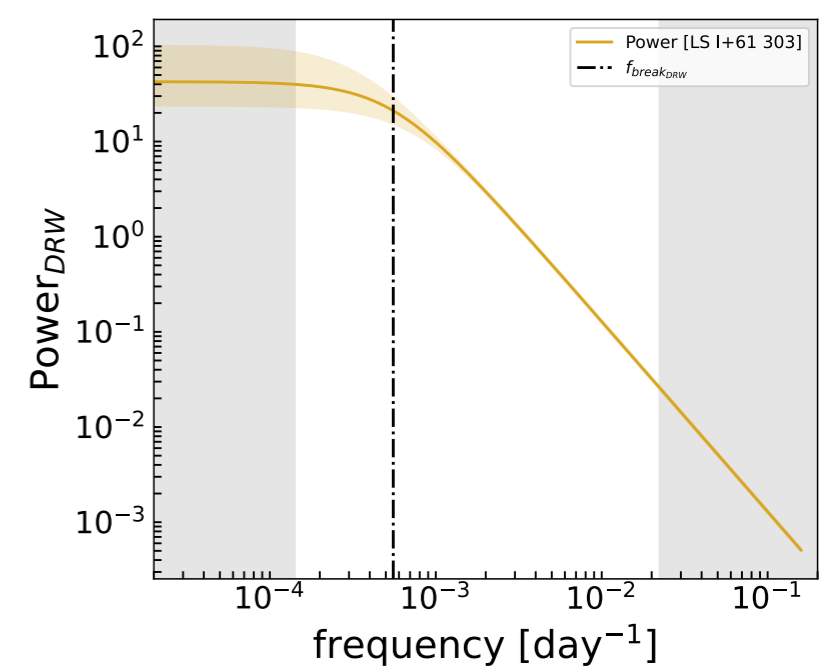
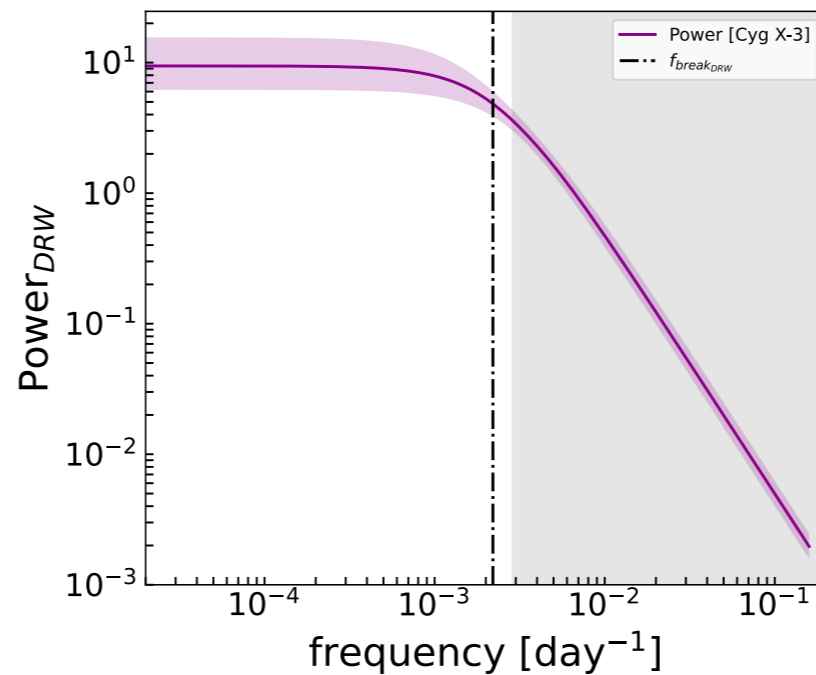
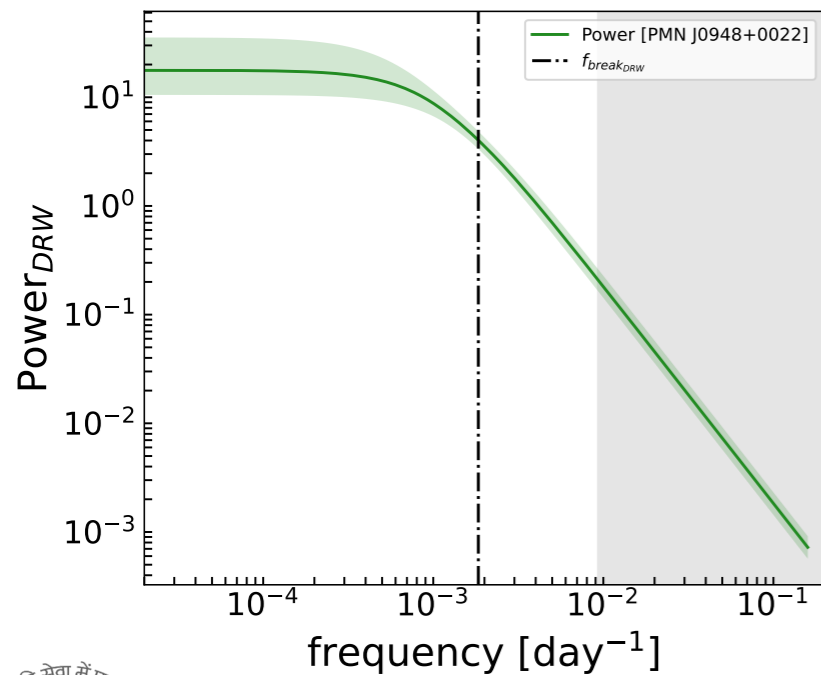
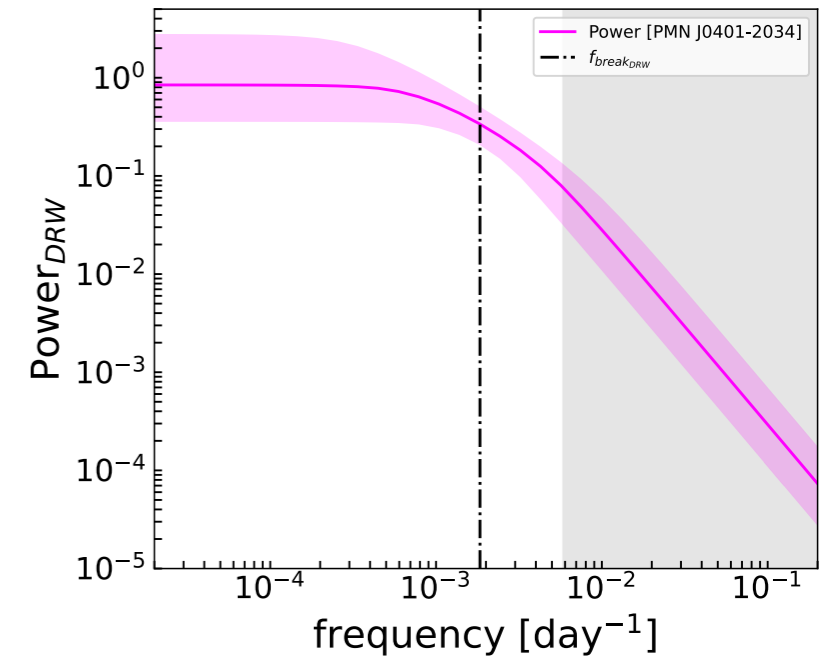
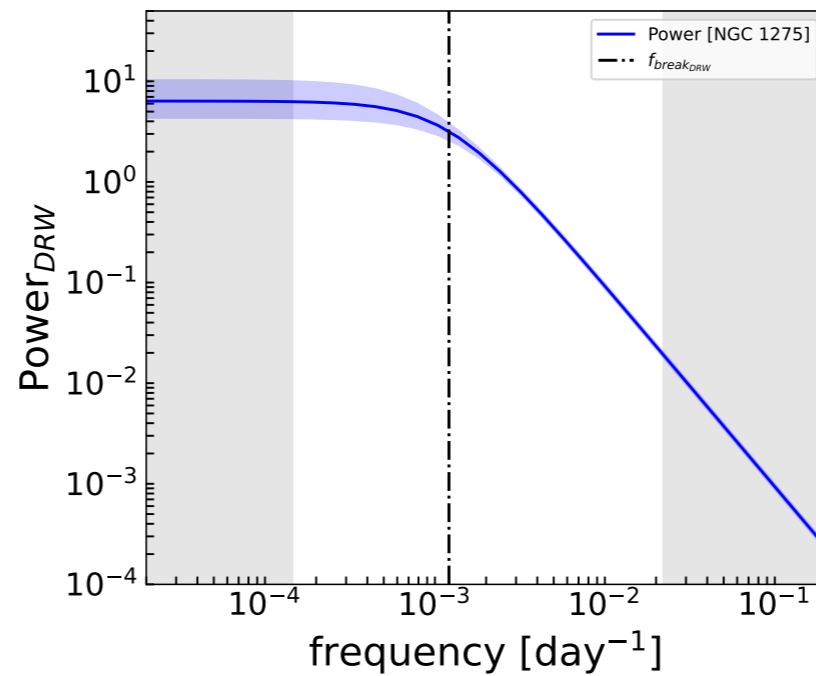
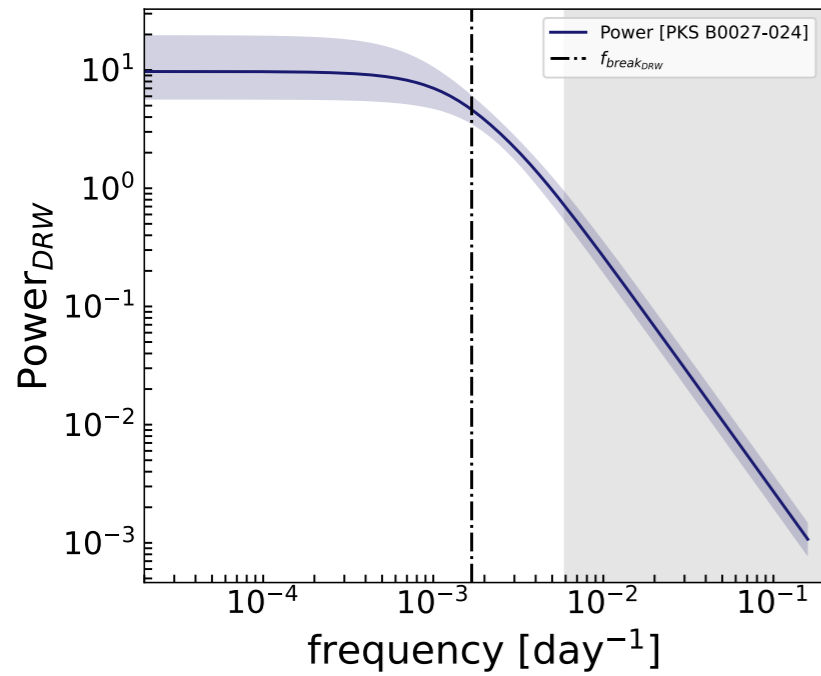
# DRW modeling

\* Marginal posterior parameter distributions of non-blazars and microquasars:



# DRW modeling

\* DRW PSD profiles of non-blazars and microquasars:



# Results

TABLE I. This table provides detailed information on 11 Active Galactic Nuclei (AGNs)—including blazars (BL Lac or FSRQ), radio galaxy (RG), narrow-line Seyfert 1 galaxies (NLS1), and blazar candidates of unclassified type (BCU)—and 2 microquasars.

Source <sup>a</sup>	4FGL name <sup>b</sup>	R.A. <sup>c</sup>	Dec <sup>c</sup>	Source type <sup>d</sup>	⟨cadence⟩ <sup>e</sup> (days)	Baseline <sup>f</sup> (days)	$z$ <sup>g</sup>	$\delta_D$ <sup>h</sup>	$\log i$ <sup>i</sup> ( $M/M_\odot$ )	$\ln \sigma_{DRW}$ <sup>j</sup>	$\ln \tau_{DRW}$ <sup>j</sup> (days)	$\log_{10} \tau_{rest}$ <sup>k</sup> (days)	Normal Distribution Fitting			References		
													$\mu$ <sup>l</sup>	$\sigma$ <sup>l</sup>	KS-test <sup>m</sup> (p-value)	$z$	$\delta_D$	$M_{BH}$
S2 0109+22	J0112.1+2245	18.0243	22.7441	BLL	8.81	~5642	0.36	2.59	$8.6 \pm 0.43$	$-0.38^{+0.15}_{-0.12}$	$5.26^{+0.33}_{-0.26}$	$2.67^{+0.14}_{-0.11}$	$0.032 \pm 0.027$	$0.26 \pm 0.022$	1.0	(1)	(2)	(3)
PKS 0735+17	J0738.1+1742	114.531	17.7053	BLL	10.58	~5621	0.424	4.5	$8.4 \pm 0.42$	$-0.42^{+0.19}_{-0.14}$	$5.52^{+0.40}_{-0.30}$	$3.39^{+0.18}_{-0.13}$	$0.033 \pm 0.019$	$0.21 \pm 0.015$	0.98	(4)	(5)	(4)
B2 1215+30	J1217.9+3007	184.467	30.1168	BLL	8.47	~5628	0.13	1.1	$8.12 \pm 0.41$	$-0.54^{+0.19}_{-0.14}$	$5.55^{+0.42}_{-0.32}$	$3.54^{+0.18}_{-0.15}$	$0.0422 \pm 0.025$	$0.311 \pm 0.020$	0.92	(6)	(5)	(7)
B3 1343+451	J1345.5+4453	206.388	44.8832	FSRQ	13.59	~5586	2.534	12.6	$8.98 \pm 0.99$	$-0.32^{+0.16}_{-0.12}$	$5.30^{+0.34}_{-0.27}$	$2.85^{+0.15}_{-0.12}$	$-0.0002 \pm 0.007$	$0.09 \pm 0.006$	0.989	(8)	(9)	(10)
S4 1726+45	J1727.4+4530	261.865	45.511	FSRQ	20.81	~5621	0.717	13.4	$8.22 \pm 0.411$	$-0.42^{+0.15}_{-0.12}$	$5.14^{+0.37}_{-0.31}$	$3.11^{+0.16}_{-0.13}$	$-0.006 \pm 0.009$	$0.144 \pm 0.007$	0.66	(11)	(9)	(12)
S5 1803+78	J1800.6+7828	270.19	78.4678	BLL	8.40	~5642	0.68	5.97	$8.6 \pm 0.43$	$-0.04^{+0.06}_{-0.06}$	$3.69^{+0.14}_{-0.13}$	$2.53^{+0.10}_{-0.08}$	$-0.008 \pm 0.0007$	$0.033 \pm 0.0005$	0.167	(13)	(13)	(14)
PKS 2052-47	J2056.2-4714	314.068	-47.2466	FSRQ	11.83	~5481	1.49	17.1	$7.88 \pm 0.39$	$-0.29^{+0.11}_{-0.09}$	$4.58^{+0.23}_{-0.20}$	$2.83^{+0.10}_{-0.09}$	$-0.011 \pm 0.007$	$0.10 \pm 0.006$	0.299	(15)	(15)	(16)
PKS B0027-024	J0030.6-0212	7.6326	-2.1989	BCU	26.78	~3696	1.804	10.3	$8.19 \pm 0.57$	$-0.45^{+0.15}_{-0.13}$	$4.55^{+0.42}_{-0.36}$	$2.64^{+0.18}_{-0.16}$	$-0.006 \pm 0.020$	$0.168 \pm 0.017$	0.786	(17)	(9)	(18)
NGC 1275	J0319.8+4130	49.9507	41.5117	RG	7.20	~5495	0.0176	1.4	$7.2 \pm 0.44$	$-0.48^{+0.12}_{-0.10}$	$4.88^{+0.26}_{-0.22}$	$2.25^{+0.12}_{-0.09}$	$0.004 \pm 0.003$	$0.108 \pm 0.002$	0.98	(20)	(20)	(20)
PMN J0401-2034	J0401.9-2034	60.4696	-20.5861	BCU	27.17	~3479	1.647	13.1	$8.19 \pm 0.57$	$-1.26^{+0.19}_{-0.18}$	$4.46^{+1.04}_{-0.82}$	$2.62^{+0.45}_{-0.36}$	$-0.042 \pm 0.024$	$0.215 \pm 0.02$	0.73	(19)	(9)	(18)
PMN J0948+0022	J0948.9+0022	147.239	0.3737	NLS1	17.11	~5042	0.5846	2.7	$7.22 \pm 0.32$	$-0.40^{+0.15}_{-0.12}$	$5.05^{+0.38}_{-0.31}$	$2.50^{+0.17}_{-0.13}$	$-0.025 \pm 0.009$	$0.116 \pm 0.007$	0.786	(21)	(27)	(21)
Cyg X-3	J2032.6+4053	308.107	40.9577	Microquasar	55.31	~5642	0.003	1.78	$0.38 \pm 0.26$	$-0.31^{+0.11}_{-0.10}$	$4.24^{+0.29}_{-0.26}$	$1.83^{+0.12}_{-0.11}$	$0.003 \pm 0.005$	$0.035 \pm 0.004$	0.351	(22)	(25)	(23)
LS I+61 303	J0240.5+6113	40.1319	61.2293	Microquasar	7.13	~5620	0.0013	1.78	$0.6 \pm 0.2$	$-0.28^{+0.21}_{-0.15}$	$5.66^{+0.42}_{-0.30}$	$2.45^{+0.18}_{-0.13}$	$-0.001 \pm 0.007$	$0.263 \pm 0.006$	0.999	(24)	(25)	(26)

**References:** (1) Collaboration *et al.* (2018), (2) Fan *et al.* (2013), (3) Zhang *et al.* (2023a), (4) Chai *et al.* (2012), (5) Liodakis *et al.* (2017a), (6) Furniss *et al.* (2019), (7) Valverde *et al.* (2020), (8) Sahakyan *et al.* (2020), (9) Chen (2018), (10) Zhang *et al.* (2024b), (11) Costamante *et al.* (2018), (12) Xiong and Zhang (2014), (13) Ghisellini *et al.* (2010), (14) Lin *et al.* (2017), (15) Wang *et al.* (2022), (16) Kadowaki *et al.* (2015), (17) Peña-Herazo *et al.* (2021), (18) Xiao *et al.* (2022), (19) <https://ned.ipac.caltech.edu> (20) Zhang *et al.* (2022), (21) Xin *et al.* (2022), (22) Koljonen and Tomsick (2020), (23) Zdziarski *et al.* (2013), (24) <https://simbad.u-strasbg.fr/simbad/sim-fbasic> (25) Molina *et al.* (2019), (26) Massi *et al.* (2017), (27) Doi *et al.* (2019).

<sup>a</sup> Source Name

<sup>b</sup> 4FGL Name

<sup>c</sup> Source Right Ascension (R.A.) and Declination (Dec.)

<sup>d</sup> Source from different classes

<sup>e</sup> Mean cadence in days

<sup>f</sup> Duration of the light curve in days

<sup>g</sup> Redshift

<sup>h</sup> Doppler factor

<sup>i</sup> Logarithm of Black Hole Mass

<sup>j</sup> Posterior parameters of modeling the Lightcurves with the DRW process

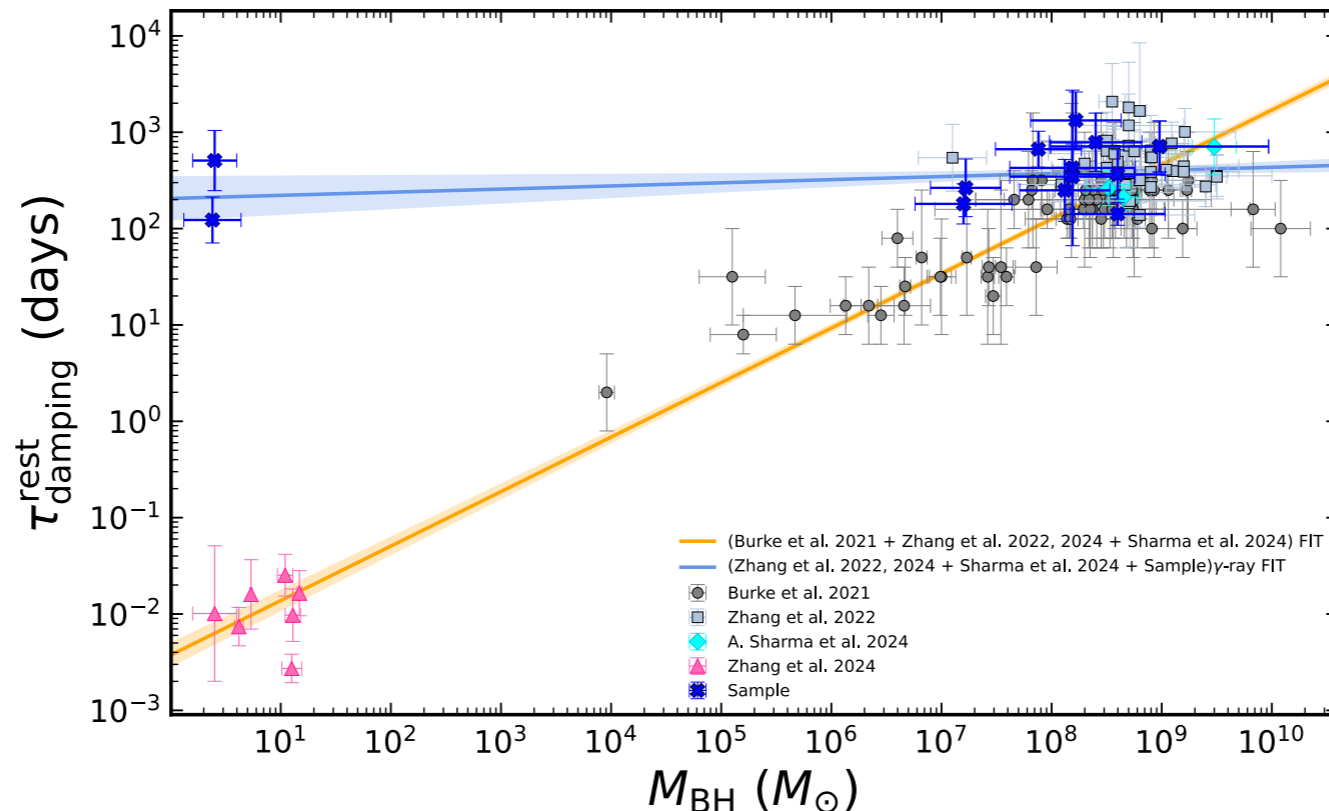
<sup>k</sup> Logarithm of damping timescale in the rest frame (days)

<sup>l</sup> Parameters of the Normal distribution fitted to the residuals

<sup>m</sup> Kolmogorov–Smirnov (KS) Test result

# Results

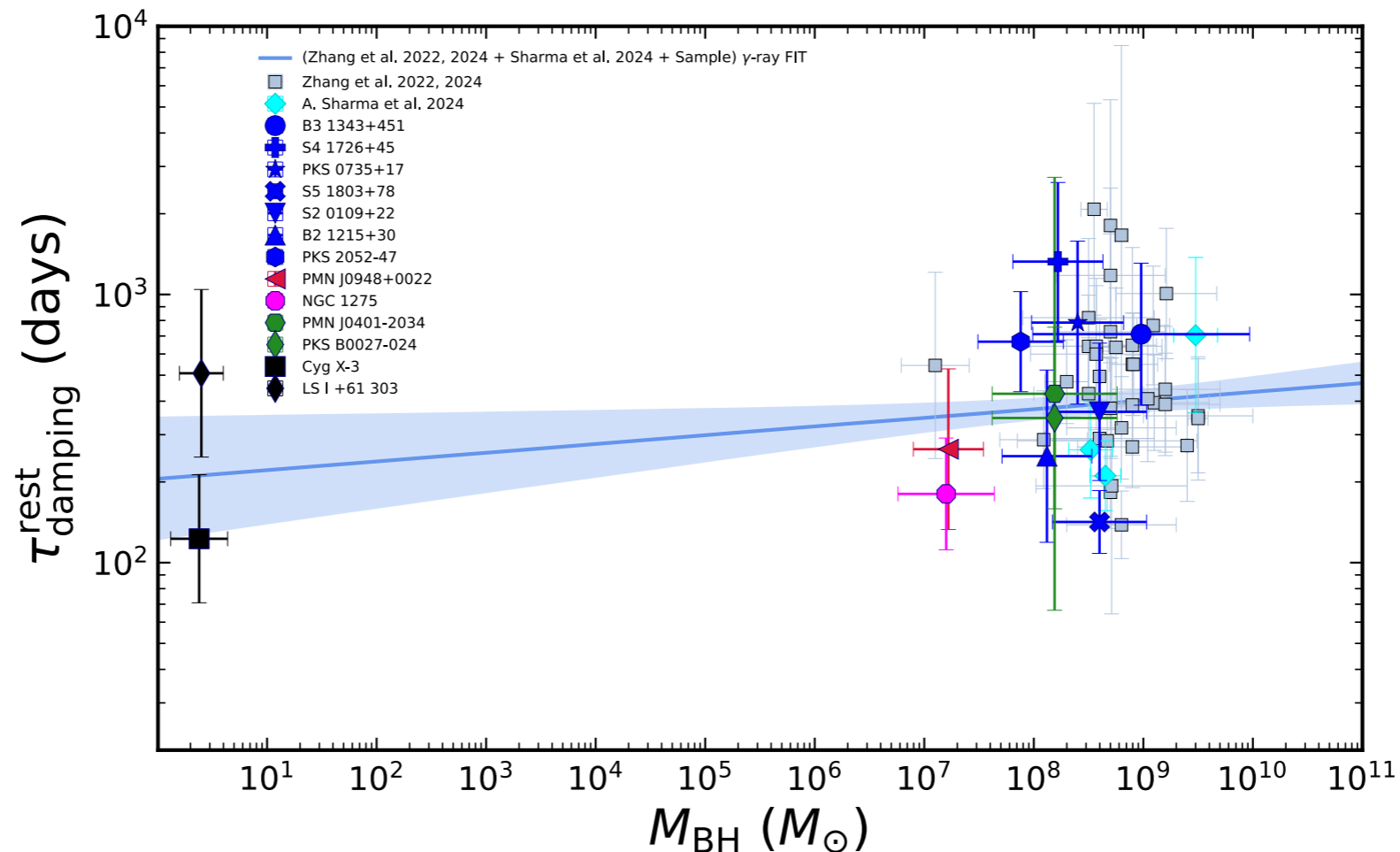
- \* In **Burke et al. 2021**, using optical data a strong correlation was observed in terms of the relation  $\tau_{damping} - M_{BH}$  and the correlation parameter is sufficiently well constrained to provide BH mass estimates using optical variability.
- \* In **Zhang et al. 2022,2024 + Sharma et al. 2024**, observed damping timescale for AGN using gamma-rays, occupy the same space as optical timescale obtained from accretion disk. This implies that the jet variability is somehow connected with accretion variability.
- \* The  $\tau_{damping} - M_{BH}$  relation also following by the x-ray variability of microquasars, **Zhang et al. 2024**.



# Results

\* In this study, the observed gamma-ray variability timescale of AGNs occupy the same space as optical variability, but in case of microquasars, the observed gamma-ray damping timescale do not follow the  $\tau_{damping} - M_{BH}$  relation.

\* The observed damping timescale of microquasars is comparable with AGNs damping timescales. This study hints at a new perspective that the relativistic jets' properties or their production mechanisms may be independent of the black hole mass.



# Conclusion

- Our findings indicate that the observed characteristic variability timescales for both AGNs and microquasars are remarkably similar, irrespective of their black hole masses.
- This suggests that common underlying processes may be responsible for the observed variations in  $\gamma$ -ray emissions across these sources.
- The same variability time scale in stellar black holes and supermassive black holes suggests the jet possibly can be produced by a similar procedure.



# Acknowledgement

I would like to thank Prof. Debanjan Bose and Prof. Raj Prince for their guidance throughout these project and to Prof. Sakuntala Chatterjee for providing the essential support needed to complete the project.

**To know more**  
**Scan me**



**Thank you**

Thank you